Nanobody-dependent delocalization of endocytic machinery in Arabidopsis root cells dampens their internalization capacity

Joanna Winkler[1,2,*], Andreas De Meyer[1,2,*], Evelien Mylle[1,2], Peter Grones[1,2], Daniël Van Damme[1,2,#]

[1]Ghent University, Department of Plant Biotechnology and Bioinformatics, Technologiepark 71, 9052 Ghent, Belgium

[2]VIB Center for Plant Systems Biology, Technologiepark 71, 9052 Ghent, Belgium

[*]equal contribution

[#]**Correspondence:**
Daniel Van Damme
daniel.vandamme@psb.vib-ugent.be

Keywords: nanobody, endocytosis, Arabidopsis, protein delocalization, fluorescence microscopy

Abstract

Plant cells perceive and adapt to an ever-changing environment by modifying their plasma membrane (PM) proteome. Whereas secretion deposits new integral membrane proteins, internalization by endocytosis removes membrane proteins and associated ligands, largely with the aid of adaptor protein complexes and the scaffolding molecule clathrin. Two adaptor protein complexes function in clathrin-mediated endocytosis at the PM in plant cells, the heterotetrameric Adaptor Protein 2 (AP-2) complex and the octameric TPLATE complex (TPC). Whereas single subunit mutants in AP-2 develop into viable plants, genetic mutation of a single TPC subunit causes fully penetrant male sterility and silencing single subunits leads to seedling lethality. To address TPC function in somatic root cells, while minimizing indirect effects on plant growth, we employed nanobody-dependent delocalization of a functional, GFP-tagged TPC subunit, TML, in its respective homozygous genetic mutant background. In order to decrease the amount of functional TPC at the PM, we targeted our nanobody construct to the mitochondria and fused it to TagBFP2 to visualize it independently of its bait. We furthermore limited the effect of our delocalization to those tissues that are easily accessible for live-cell imaging by expressing it from the PIN2 promotor, which is active in root epidermal and cortex cells. With this approach, we successfully delocalized TML from the PM. Moreover, we also show co-recruitment of TML-GFP and AP2A1-TagRFP to the mitochondria, suggesting that our approach delocalized complexes, rather than individual adaptor complex subunits. In line with the specific expression domain, we only observed minor effects on root growth and gravitropic response, yet

realized a clear reduction of endocytic flux in epidermal root cells. Nanobody-dependent delocalization in plants, here exemplified using a TPC subunit, has the potential to be widely applicable to achieve specific loss-of-function analysis of otherwise lethal mutants.

1 Introduction

Cells are delineated by their plasma membrane (PM). The PM houses a plethora of proteins ranging from receptors and ion channels to structural membrane proteins. Many of these PM proteins, commonly termed cargo, are responsible for cellular communication with the outside world. In eukaryotes, endocytosis is the cellular process where cargoes, associated ligands as well as lipids are internalized from the PM. Endocytosis thereby provides a way to regulate the content and consequently modulate protein activity at the PM. A predominant and well-studied form of endocytosis is clathrin-mediated endocytosis (CME) (Bitsikas et al., 2014). CME refers to the dependency of the scaffolding protein clathrin, which coats the developing and mature vesicles (Robinson, 2015). In plants, CME plays a role in hormone signaling (Irani et al., 2012; Martins et al., 2015; Zhang et al., 2017), nutrient availability (Wang et al., 2017; Dubeaux et al., 2018; Yoshinari et al., 2019), pathogen defense and susceptibility (Mbengue et al., 2016; Li and Pan, 2017), and other biotic and abiotic stresses (Li et al., 2011). Consequently, CME is essential for plant development.

Two early-arriving adaptor complexes, the heterotetrameric Adaptor Protein-2 complex (AP-2) and the hetero-octameric TPLATE complex (TPC) facilitate CME in plants. In contrast to AP-2, TPC represents an evolutionary ancient protein complex, which is lost in yeast and mammalian cells (Hirst et al., 2014). The slime mold *Dictyostelium discoideum* contains a similar complex, named TSET. TSET however is a hexameric complex in contrast to TPC in *A. thaliana*, which has two additional subunits. Also contrary to TPC, TSET is dispensable in *D. discoideum* (Hirst et al., 2014). The presence of a full or partial TSET complex in other eukaryotes was confirmed by additional homology searches, indicative of its ancient evolutionary origin (Hirst et al., 2014).

AP-2 and TPC have both common and distinct functions, possibly relating to cargo specificity and/or fate of the internalized cargo (Bashline et al., 2015; Sánchez-Rodríguez et al., 2018; Wang et al., 2019; Yoshinari et al., 2019). In addition, functional diversification of both complexes is reflected in their mutant phenotypes. Knockout plants in individual AP-2 subunits are affected at various stages of development but viable (Di Rubbo et al, 2013; Kim et al, 2013; Fan et al, 2013; Yamaoka et al, 2013; Bashline et al, 2013). However, *ap2* mutants show reduced internalization of the styryl dye FM4-64, which can be seen as proxy to a difference in cargo uptake (Jelínková et al., 2010), as well as known

endocytic cargoes like the brassinosteroid receptor BRASSINOSTEROID INSENSITIVE 1 (BRI1), the Boron exporter BOR1 and auxin efflux carriers of the PIN family (Di Rubbo et al., 2013; Fan et al., 2013; Kim et al., 2013; Yoshinari et al., 2016, 2019).

The relatively mild phenotype of *ap2* single subunit mutants in plants contrasts with the lethal phenotype of a single *ap2* subunit knockout in mice (Mitsunari et al., 2005). Alternatively, the complex does not seem to be essential for yeast (Yeung et al., 2013). In *Caenorhabditis elegans,* AP-2 subunits are capable of assembling into hemicomplexes which partially retain their functionality (Gu et al., 2013). In plants, AP2M and AP2S are still recruited to the PM in *ap2s* and *ap2m* mutants respectively (Wang et al., 2016), suggesting that AP-2 hemicomplexes might also confer partial functionality in plants.

In contrast to AP-2, single knockouts of TPC subunits result in fully penetrant male sterility with shriveled pollen and ectopic callose accumulation (Van Damme et al., 2006; Gadeyne *et al*, 2014). Similar pollen-lethal phenotypes are also reported for *drp1c* (Backues et al., 2010) as well as *clc1* (Wang et al., 2013), involved in vesicle fission and clathrin triskelion assembly respectively.

So far, there is only one viable weak allele of one TPC subunit identified. This *twd40-2-3* mutant (Bashline et al., 2015) is however likely merely a knockdown as *twd40-2-1* and *twd40-2-2* mutants are pollen lethal (Gadeyne et al., 2014). Knockdowns of *TML* and *TPLATE* resulted in seedling lethality with a reduced internalization of FM4-64, BRI1, RECEPTOR-LIKE PROTEIN 44 (RLP44) and the cellulose synthase subunit CESA6 (Irani et al., 2012; Gadeyne et al., 2014; Sánchez-Rodríguez et al., 2018; Gómez et al., 2019). Silencing works on the messenger level and phenotypes only become apparent following degradation of pre-made proteins. As adaptor protein complexes can be recycled following each round of internalization, approaches affecting these complexes at the protein level have a more direct effect. In animal cells, conditional delocalization using rapamycin to target AP-2 to mitochondria has been successfully applied to interfere with endocytosis (Robinson et al., 2010).

Since their discovery, nanobodies, derived from camelid heavy chain-only antibodies (HCAb), have found their way into a wide variety of applications in biological fields. Nanobodies are similar to antibodies (Ab) in the sense that they can bind epitopes with high affinity in a highly selective manner (Ingram et al., 2018). Their applications range from drug discovery, crystallography and imaging techniques to probing protein functions (Ingram et al., 2018). The latter can be done by enforcing nanobody-dependent protein degradation or nanobody-dependent localization (Caussinus et al., 2012; Früholz et al., 2018; Ingram et al., 2018). Nanobodies can be expressed as a single chain, compact and

stable protein while still retaining high selectivity and affinity for its epitope (Muyldermans, 2013). This makes them more convenient to clone and to express compared to conventional antibodies.

A nanobody-dependent method, degradFP, was developed in *Drosophila melanogaster*, to generate a conditional knockout at the protein level. This tool uses an anti-GFP nanobody, linked to an F-box to target it for ubiquitin-dependent degradation (Caussinus et al., 2012). This approach has also very recently been successfully used in plants to degrade WUSCHEL-GFP (Ma et al., 2019). Nanobodies have also been used in Arabidopsis seedlings to lock down vacuolar sorting receptors (VSRs) in cellular compartments upstream of TGN/EE, allowing to determine their retrograde trafficking pathway (Früholz et al., 2018).

Finally, nanobody-dependent lockdown was successfully applied in HeLa cells where EPS15, a pioneer endocytic accessory protein (EAP) that facilitates initiation of CME by stabilizing AP-2 presence at the PM, was successfully delocalized by expressing an anti-EPS15 nanobody on endosomes or mitochondria, thereby inactivating it (Traub, 2019).

Lock down of proteins to a cellular compartment of choice and can thus be effectively used in a similar fashion as the rapamycin-based system from the Robinson lab (Robinson et al., 2010). Here, we explore the effects on CME by delocalizing a GFP-tagged functional TML-GFP fusion protein to the mitochondria in the homozygous *tml-1(-/-)* mutant background using an nanobody directed against eGFP.

2 Results

2.1 A mitochondrially targeted nanobody can delocalize TML

TPC is a robust multi-subunit complex functioning at the PM and TPC can be affinity purified using any of its subunits as bait (Gadeyne et al., 2014). In order to delocalize, and thereby inactivate TPC, we took advantage of the functionally complemented homozygous *tml-1*(-/-) mutant expressing TMLprom::TML-GFP (Gadeyne et al., 2014). In this background, we introduced expression of a nanobody directed against eGFP (GFPNb) (Künzl et al., 2016), which we visualized by fusing it to TagBFP2. We targeted the fusion protein to the mitochondria using the import signal of the yeast mitochondrial outer membrane protein Tom70p as described before (Robinson et al., 2010). This targeting signal is functional in plants as we have previously colocalized constructs containing this signal with mitoTracker in *N. benthamiana* leaf epidermal cells (Winkler et al., unpublished results). We used the PIN2prom to drive expression of MITOTagBFP2-GFPNb in epidermis and cortex root

files, which are easy to image with respect to future experiments. MITOTagBFP2-GFPNb localized to discrete punctae in Arabidopsis wild type roots (**Figure 1A**). These punctae appeared to have different sizes, with the large ones likely representing clusters. Co-staining with the mitochondrial dye MitoTracker Red revealed hardly any colocalization (**Figure 1A**), which might suggest that expression of MITOTagBFP2-GFPNb has an effect on mitochondrial fitness. Nevertheless, we used this tool to attempt to delocalize TML away from the PM.

In complemented *tml-1*(-/-) Arabidopsis roots, TML-GFP is recruited predominantly at the plasma membrane in a single confocal section (**Figure 1B**). Combining this line with the GFPNb, whose expression was restricted to the root epidermis and cortex files (**Figure 1C**), led to a change in the uniform plasma membrane labeling of TML to a denser staining of discrete punctae in these cell files. Most of those were still near the plasma membrane and colocalized with the fluorescent signal from the nanobody, indicating effective delocalization of TML-GFP (**Figure 1C and enhanced in 1D**). This delocalization was not apparent in the deeper layers of the root, where TML remained uniformly recruited to the plasma membrane (**Figure 1C**). Detailed analysis using spinning disk microscopy confirmed the strong recruitment of TML to those mitochondria that were present in the focal plane of the PM (**Figure 1E and 1F, arrowheads**). Next to the mitochondria however, TML was still recruited to endocytic foci at the plasma membrane in root epidermal cells. The density of endocytic foci in epidermal root cells is very high (Dejonghe et al., 2016, 2019; Sánchez-Rodríguez et al., 2018) and the density of endocytic foci, marked by TML-GFP, appeared similar between epidermal cells in the complemented mutant (control) background and in those cells that in addition also expressed GFPNb. The fluorescence intensity of the foci was however markedly reduced, in agreement with a substantial amount of TML-GFP accumulating at the mitochondria (**compare Figure 1E and 1F**).

2.2 Nanobody-dependent delocalization of TML also affects other endocytic players

In plants, the heterotetrameric AP-2 complex and the octameric TPLATE complex are presumed to function largely, but not exclusively, together to execute CME (Gadeyne et al., 2014; Bashline et al., 2015; Wang et al., 2016; Adamowski et al., 2018). Both TPC and AP-2 have been shown to be involved in the internalization of cellulose synthase (CESA) complexes or the Brassinosteriod receptor BRI1 for example (Bashline et al., 2013, 2015; Di Rubbo et al., 2013; Gadeyne et al., 2014; Sánchez-Rodríguez et al., 2018).

Moreover, a joint function is also suggested from proteomics analyses, which could identify subunits of both complexes when the AtEH1/Pan1 TPC subunit was used as bait in tandem-affinity purification assays (Gadeyne et al., 2014). To investigate whether our tool, aimed at delocalizing TPC, would also

interfere with AP-2 recruitment at the PM, we tested the localization of AP-2 when TML was targeted to the mitochondria. To do so, we crossed our TML-GFP line, *in tml-1*(-/-) and expressing PIN2prom::MITOTagBFP2-GFPNb with the homozygous complemented *tml-1*(-/-) line, expressing TML-GFP as well as one of the large AP-2 subunits, AP2A1, fused to TagRFP (Gadeyne et al., 2014). Offspring plants that did not inherit the nanobody construct showed PM and cell plate recruitment of TML and AP2A1, and only background fluorescence in the TagBFP2 channel (**Figure 2A**). In the offspring plants that inherited the nanobody construct however, the localization of the adaptor complex subunits changed. Both TML and AP2A1 accumulated at punctae, which clearly colocalized with the TagBF2-fused nanobody construct (**Figure 2B**). The observed delocalization of AP2A1 to the mitochondria, together with TML strongly suggests that our approach has the capacity to delocalize TPC and AP-2 rather than TML alone, given that TPC and AP-2 are presumed to be linked via the AtEH1/Pan1 subunit (Gadeyne et al., 2014).

2.3 Mistargeting adaptor complexes in epidermis and cortex affects root endocytic uptake with only minor effects on root growth.

In contrast to AP-2, genetic interference with TPC subunits causes fully penetrant male sterility (Van Damme et al., 2006; Di Rubbo et al., 2013; Fan et al., 2013; Kim et al., 2013; Yamaoka et al., 2013; Gadeyne et al., 2014). TPC functionality therefore requires all subunits, and constitutive homozygous loss-of-function backgrounds are therefore non-existing. Abolishing endocytosis in plants, by silencing TPC subunits (Gadeyne et al., 2014) or over expression of the uncaging proteins AUXILLIN-LIKE 1 or 2 (Adamowski et al., 2018) severely affects seedling development. The effect of silencing TPC subunits only indirectly affects protein levels and targeting clathrin might interfere with trafficking at endosomes besides the PM. As TPC and AP-2 only function at the PM, inactivating their function should not directly interfere with more downstream aspects of endosomal trafficking. Furthermore, by restricting the expression domain where adaptor complex function is tuned-down to the two outermost layers in the root should allow to study internalization from the PM, independently of possible indirect effects caused by the severe developmental alterations.

Visual inspection of seedlings, grown vertically on plates before imaging did not reveal any major developmental arrest (**Figure 3A**). Root growth measurements of seedlings expressing either GFPNb alone, or GFPNb combined with TML-GFP in the complemented *tml-1(-/-)* mutant background grew similarly. There was a slight reduction in average root length when WT (Col-0) seedlings, grown in continuous light, were compared to WT plants expressing MITOTagBFP2-GFPNb. This was also quantifiable in the complemented mutant background (**Figure 3B, left**), indicating that this was caused

by GFPNb expression, rather than TML sequestration. Partial delocalization of TML therefore does not impair root growth under normal growth conditions. The AtEH/Pan1 TPC subunits were recently implicated in growth under nutrient-depleted conditions as downregulation of *AtEH1/Pan1* expression rendered plants hyper-susceptible to for example carbon starvation (Wang et al., 2019). We therefore assessed if delocalizing TML-GFP, as well as other endocytic players, would also render these plants susceptible nutrient stress. To do so, we used the seedlings, grown for five days in continuous light. We placed them in the dark for an additional seven days and measured root lengths. We observed only minor differences. The GFPNb expressing plants showed a mild root growth reduction compared to the WT control (**Figure 3B, middle**), similar to what was observed in the light (**Figure 3B, left**). This difference was however not as outspoken in the complemented mutant background, indicating that partial delocalization of TML in epidermis and cortex cells had a mildly positive effect on root growth in the dark. Comparing root growth in the light and in the dark for every individual seedling allowed to equalize out the effect of GFPNb expression. This lead to similar ratios in the WT background while amplifying the effect of partial TML delocalization (**Figure 3B, right**). Nevertheless, the effects of TML relocalization on root growth were mild, which was also confirmed in a gravistimulation experiment. We followed the gravitropic response of 5 days old seedling for 12 hours and observed only minor differences in root bending following gravistimulation in the seedlings with partial TML delocalization than those from the complemented mutant line (**Figure 3C and 3D**).

The subtle differences observed by comparing the effect of delocalization of TML on plant growth are likely a consequence of the restricted expression domain of GFPNb. We therefore monitored the effects of delocalizing TML more directly by visualizing the internalization of the styryl dye FM4-64, which in plants is commonly used as proxy for endocytic flux (Rigal et al., 2015; Jelínková et al., 2019). To rule out indirect effects of targeting GFPNb to the mitochondria, we compared endocytic flux between WT (Col-0) expressing MITOTagBFP2-GFPNb, TML-GFP *in tml-1(-/-)* and two independent lines of TML-GFP in *tml-1(-/-)* expressing MITOTagBFP2-GFPNb. We observed a slight decrease in endocytic flux when comparing wild type seedlings with the complemented *tml-1(-/-)* line and a strong reduction in endocytic flux between the complemented mutant and both complemented mutant lines where TML was partially delocalized. Direct visualization of endocytic flux therefore allowed us to conclude that expression of the PIN2prom::MITOTagBFP2-GFPNb has the capacity to interfere with endocytosis in Arabidopsis root epidermal cells and that this tool certainly has the capacity to generate knockdown, and maybe even knockout lines at the protein level.

3 Discussion

Analyzing how impaired TPC function directly affects endocytosis is hampered by the male sterility and/or seedling lethal mutant phenotypes following genetic interference of individual subunits (Gadeyne et al., 2014). Here, we explored to impair TPC function at the protein level by delocalizing a functional and essential subunit in its respective complemented mutant background. We were inspired by previous work in animal cells. However, instead of using rapamycin-dependent rerouting of one of the large AP-2 subunits, combined with silencing the endogenous subunit (Robinson et al., 2010), we took advantage of the complemented *tml-1(-/-)* mutant line expressing TML-GFP (Gadeyne et al., 2014) in combination with targeting a nanobody directed against GFP (GFPNb) (Künzl et al., 2016) to the mitochondria. We expressed the GFPNb in epidermis, cortex and lateral root cap as we expected ubiquitous constitutive expression to be lethal for the plant. Moreover, the epidermis and cortex cell files are easily accessible for imaging purposes. Proteins fused to this mitochondrial targeting signal colocalized with MitoTracker in transient *N. benthamiana* experiments (Winkler et al., unpublished results). This was not the case in Arabidopsis roots, indicating that constitutively decorating the mitochondria with the GFPNb construct affected their functionality without however causing a severe penalty on overall plant growth. The GFPNb system was capable of delocalizing TML-GFP and this caused the appearance of strongly fluorescent GFP-positive aggregations. Detailed inspection revealed however that our approach was insufficient to remove all TML from the PM. Compared to the control cells, sequestration of TML-GFP led to an overall reduction in signal intensity at the endocytic foci, without visually affecting their overall density. This also correlated with a significant reduction in endocytic tracer uptake, a proxy for reduced endocytosis. Intuitively, a reduced amount of complexes per endocytic spot would correlate with a weaker signal rather than a reduction in density. Our observation therefore fits with the occurrence and requirement of several TPC units to efficiently internalize a single clathrin coated vesicle.

The minor differences in root length, observed when TML-GFP was delocalized in the GFPNb lines, as well as the minor effects observed upon gravistimulation can be explained by the limited expression domain of the PIN2 promoter. Nevertheless, the observed effects are weak when compared to disrupting other parts of the CME machinery. Inducible overexpression of AUXILIN-LIKE1/2 results in complete seedling growth arrest with drastic effects on cell morphology (Adamowski et al., 2018). The same holds true for inducible expression of dominant-negative clathrin HUB and DRP1A (Kitakura et al., 2011; Yoshinari et al., 2016). Furthermore, estradiol-inducible TPLATE and TML knockdown lines are noticeably shorter, show less gravitropic capacity and also show bulging cells

(Gadeyne et al., 2014). As we did not observe cellular effects in epidermal or cortical cell files, we conclude that our approach lacked the required strength to block endocytosis, but only reduced it.

Recent results suggest that plant cells very likely contain a feedback loop controlling TPC expression, as carbon starved plants contained roughly the same amount of full-length TPLATE-GFP, next to an extensive amount of TPLATE-GFP degradation products (Wang et al., 2019). In case plant cells make more TPC upon depleting the complex at the PM, DegradFP could provide a viable solution to this problem (Caussinus et al., 2012). By applying this method in GFP-complemented *tml-1(-/-)* mutants, newly synthesized TML-GFP would be broken down immediately, preventing to achieve functional levels of TPC at the PM. Stronger or inducible promotors and/or the use of a different targeting location might also increase the delocalization capacity. To avoid lethality due to ubiquitous sequestration, engineered anti-GFP nanobodies, whose affinity can be controlled by small molecules, could also be used (Farrants et al., 2020).

Untangling the function of TPC and AP-2 in CME at the plasma membrane requires tools that allow interfering specifically with the functionality of both complexes. Our nanobody-dependent approach targeting TPC via TML resulted in the co-delocalization of one of the large subunits of AP-2, indicating that we likely are not only targeting TPC, but also AP-2 function. Whether a complementary approach, by delocalizing AP-2, using AP2S or AP2M in their respective complemented mutant backgrounds, would also delocalize TPC is something that would be worth trying. Furthermore, as AP2S and AP2M subunits are still recruited in *ap2m* and *ap2s* single mutant backgrounds (Wang et al., 2016), AP-2 in plants might also function as hemi-complexes similar to what is reported in *C. elegans* (Gu et al., 2013). Single mutants therefore might do not reflect functional null *ap2* mutants and a similar approach as performed here might also provide tools to inactivate AP-2 as a whole, which can be highly complementary to working with the single subunit mutants.

In conclusion, the data presented here is a first step toward the development of specific tools, which are required to help us understand the functions of AP-2 and TPC. On the long-term, this will generate insight into endocytosis at the mechanistic level and this will bring us closer to being able to modulate CME-dependent processes, and thereby modulating plant development, nutrient uptake as well as defense responses to our benefit.

4 Materials and Methods

4.1 Cloning

Gateway entry clones pDONR221-TagBFP2, pDONR221-MITOTagBFP2 and pDONRP2RP3-GFPNb were generated according to the manufacturer's instructions (ThermoFisher Scientific BP clonase). pDONR221-TagBFP2 was amplified from pSN.5 mTagBFP2 (Pasin et al., 2014) with primers:

AttB1-GGGGACAAGTTTGTACAAAAAAGCAGGCTATGTCATCTAAGGGTGAAGAGCTTATCAAAGAGAAT and AttB2-GGGGACCACTTTGTACAAGAAAGCTGGGTCACCTCCGCCACCTCCACCTCCCAGTCCTGCGTA.

pDONR221-MITOTagBFP2 was generated from pDONR221-TagBFP2 by including the import signal of the yeast mitochondrial outer membrane protein Tom70p as described before (Robinson et al., 2010). The following primers sequences were used:

AttB1-GGGGACAAGTTTGTACAAAAAAGCAGGCTCAATGAAGAGCT TCATTACAAGGAACAAGACAGCCATTTTGGC AACCGTTGCTGCTACAGGTACTGCCATCGGTGCCTACTATTATTACAACCAATTGCAACAGGATCCACCGGTCGCCACC ATGTCATCTAAGGGTGAAGAGCTT and AttB2-GGGGACCACTTTGTACAAGAAAGCTGGGTACGCTAAGTCTTCCTCT GAAATCAA.

pDONRP2RP3-GFPNb was generated from an anti-GFP Nanobody construct (Künzl et al., 2016) with primers attB2-GGGGACAGCTTTCTTGTACAAAGTGGGGATGTATCCTTATGATGTTC and attB3r-GGGGACAACTTTGTATAATAAAGTTGTTTAATGATGATGATGATGATGAGAAGA including a HA-tag, a 3xHis-tag and a stop codon.

The entry clones of the PIN2 promoter pDONRP4P1R_PIN2prom (Marquès-Bueno et al., 2016), pDONR221-MITOTagBFP2 and pDONRP2RP3-GFPNb were used in a triple Gateway LR reaction, combining pB7m34GW (Karimi et al., 2005) to yield pB7m34GW_PIN2prom::MITOTagBFP2-GFPNb.

4.2 Plant material and transformation

Plants expressing pB7m34GW_PIN2prom::MITOTagBFP2-GFPNb were generated by floral dip (Clough and Bent, 1998). Constructs were dipped into Col-0 and *tml-1(-/-)* (At5g57460) mutant lines described previously (Gadeyne et al., 2014). Primary transformants (T1) were selected on BASTA containing ½ strength MS medium without sucrose and 0.6% Gelrite (Duchefa, The Netherlands). PIN2prom::MITOTagBFP2-GFPNb expression was analyzed in the progeny of BASTA-resistant primary transformants (T2 seeds) by microscopy and T2 lines demonstrating strong expression were

selected regardless of insert copy number. Next, T2 lines were crossed with the previously described TML-GFP complemented *tml-1(-/-)* mutant line expressing also RPS5Aprom::AP2A1-TagRFP (Gadeyne et al., 2014). Primary hybrids were analyzed via microscopy and best lines were selected on the basis of both PIN2prom::MITOTagBFP2-GFPNb and RPS5Aprom::AP2A1-TagRFP expression.

4.3 Phenotypical quantification of root growth

Arabidopsis seedlings were grown at 21°C on ½ strength MS medium without sucrose and 0.6% Gelrite (Duchefa, Netherlands). For root growth and carbon starvation, plants were grown for 5 days in continuous light upon which the root growth of every seedling was marked. Subsequently, the plates were covered and left for 7 days in dark after which root growth was marked again. For the gravistimulation assay plants were grown for 5 days in continuous light, after which the plate was turned 90°. Pictures were taken at 30-minute intervals using a Canon EOS 650D with a Canon macro lens EF 100mm and the EOS utility software (Canon Inc.). Root growth and gravitropism measurements were carried out with Fiji/ImageJ (Schindelin et al., 2012; Schneider et al., 2012). Statistical difference was determined using the Wilcoxon-signed rank test. For the root growth analysis, outliers were removed via interquartile range in a single step. Data were analyzed using Rstudio (Rstudio Team, 2019) with Welch corrected ANOVA to account for heteroscedasticity. Post hoc pairwise comparison was performed with the package MULTCOMP utilizing the Tukey contrasts (Herberich et al., 2010).

4.4 FM-uptake quantification

Endocytic tracer FM4-64 stock solution was prepared prior to treatment (2 mM in DMSO, Thermo Fisher). Roots were stained with 2 μM FM4-64 by incubating the seedlings in FM-containing ½ strength MS medium without sucrose for 30 min. Treatment was followed by microscopy. Acquired pictures were analyzed in Fiji/ImageJ (Schindelin et al., 2012; Schneider et al., 2012). PM and cytosol of individual epidermal cells were outlined (using the Select Brush Tool and Freehand selections, respectively) and histograms of pixel intensities were generated. Pictures which contained more than 1% saturated pixels were excluded from the quantification. Cytoplasm/PM ratios were calculated from average intensities of the top 1% highest intensity pixels based on the histograms. Outliers were removed via interquartile range in a single step. Data were analyzed using RStudio (Rstudio Team, 2019). Data distribution normality was check with Shapiro-Wilk test, and the significance level was tested with Wilcoxon-signed rank test for non-parametric data.

4.5 Image acquisition

Confocal images were taken using Leica SP8X confocal microscope equipped with a WLL laser and using the LASX software (Figure 1 A-D, Figure 2 and Figure 4). Images were acquired on Hybrid (HyD, gating 0.3-10.08 ns) and Photomultiplier (PMT) Detectors using bidirectional line-sequential imaging with a 40x water objective (NA=1.10) and frame or line signal averaging. Specific excitation and emission were used: 405nm laser and filter range 410-470nm for TagBFP2, 488nm laser and filter range 500-550nm for GFP, 488nm laser and filter range 600-740nm for FM4-64, 555nm laser and filter range 560-670 for TagRFP. Focal planes of plasma membranes (Figure 1E and 1F) were acquired with a PerkinElmer Ultraview spinning-disc system attached to a Nikon Ti inverted microscope and operated using the Volocity software package (Figure 1 E and F). Images were acquired on an ImagEMccd camera (Hamamatsu C9100-13) using frame-sequential imaging with a 100x oil immersion objective (NA=1.45). Specific excitation and emission was performed using a 488nm laser combined with a single band pass filter (500-550nm) for GFP and 405nm laser excitation combined with a single band pass filter (454-496nm) for TagBFP2. Images shown are single-slice.

5 Conflict of Interest

The authors declare that the research was conducted in the absence of any commercial or financial relationships that could be construed as a potential conflict of interest.

6 Author Contributions

JW, ADM, EM and PG designed and performed experiments. DVD designed experiments and wrote the initial draft together with ADM. All authors contributed to the final version of the manuscript.

7 Funding

The European Research Council (T-Rex project number 682436 to D.V.D., J.W. and A.D.M) and the Research Foundation Flanders (FWO postdoctoral fellowship grant 1226420N to P.G.).

8 Acknowledgments

The authors would like to thank the ENPER members for forming a vibrant and open research community for more than 20 years already. We would also like to thank Steffen Vanneste (PSB, VIB/UGent, Belgium) for providing research toolss. Research in the Van Damme lab is supported by the European Research Council (T-Rex project number 682436 to D.V.D., J.W. and A.D.M) and by the Research Foundation Flanders (FWO postdoctoral fellowship grant 1226420N to P.G.).

9 References

Adamowski, M., Narasimhan, M., Kania, U., Glanc, M., De Jaeger, G., and Friml, J. (2018). A Functional Study of AUXILIN-LIKE1 and 2, Two Putative Clathrin Uncoating Factors in

Arabidopsis. *Plant Cell*, tpc.00785.2017. doi:10.1105/tpc.17.00785.

Backues, S. K., Korasick, D. A., Heese, A., and Bednarek, S. Y. (2010). The Arabidopsis Dynamin-Related Protein2 Family Is Essential for Gametophyte Development . *Plant Cell* 22, 3218–3231. doi:10.1105/tpc.110.077727.

Bashline, L., Li, S., Anderson, C. T., Lei, L., and Gu, Y. (2013). The Endocytosis of Cellulose Synthase in Arabidopsis Is Dependent on 2, a Clathrin-Mediated Endocytosis Adaptin. *Plant Physiol.* 163, 150–160. doi:10.1104/pp.113.221234.

Bashline, L., Li, S., Zhu, X., and Gu, Y. (2015). The TWD40-2 protein and the AP2 complex cooperate in the clathrin-mediated endocytosis of cellulose synthase to regulate cellulose biosynthesis. *Proc. Natl. Acad. Sci.* 112, 12870–12875. doi:10.1073/pnas.1509292112.

Bitsikas, V., Corrêa, I. R., and Nichols, B. J. (2014). Clathrin-independent pathways do not contribute significantly to endocytic flux. *Elife*. doi:10.7554/eLife.03970.

Caussinus, E., Kanca, O., and Affolter, M. (2012). Fluorescent fusion protein knockout mediated by anti-GFP nanobody. *Nat. Struct. Mol. Biol.* 19, 117–122. doi:10.1038/nsmb.2180.

Clough, S. J., and Bent, A. F. (1998). Floral dip: A simplified method for Agrobacterium-mediated transformation of Arabidopsis thaliana. *Plant J.* doi:10.1046/j.1365-313X.1998.00343.x.

Dejonghe, W., Kuenen, S., Mylle, E., Vasileva, M., Keech, O., Viotti, C., et al. (2016). Mitochondrial uncouplers inhibit clathrin-mediated endocytosis largely through cytoplasmic acidification. *Nat. Commun.* 7. doi:10.1038/ncomms11710.

Dejonghe, W., Sharma, I., Denoo, B., De Munck, S., Lu, Q., Mishev, K., et al. (2019). Disruption of endocytosis through chemical inhibition of clathrin heavy chain function. *Nat. Chem. Biol.* doi:10.1038/s41589-019-0262-1.

Di Rubbo, S., Irani, N. G., Kim, S. Y., Xu, Z.-Y., Gadeyne, A., Dejonghe, W., et al. (2013). The Clathrin Adaptor Complex AP-2 Mediates Endocytosis of BRASSINOSTEROID INSENSITIVE1 in Arabidopsis. *Plant Cell* 25, 2986–2997. doi:10.1105/tpc.113.114058.

Dubeaux, G., Neveu, J., Zelazny, E., and Vert, G. (2018). Metal Sensing by the IRT1 Transporter-Receptor Orchestrates Its Own Degradation and Plant Metal Nutrition. *Mol. Cell* 69, 953–964.e5. doi:10.1016/j.molcel.2018.02.009.

Fan, L., Hao, H., Xue, Y., Zhang, L., Song, K., Ding, Z., et al. (2013). Dynamic analysis of Arabidopsis AP2 σ subunit reveals a key role in clathrin-mediated endocytosis and plant development. *Development* 140, 3826–37. doi:10.1242/dev.095711.

Farrants, H., Tarnawski, M., Müller, T. G., Otsuka, S., Hiblot, J., Koch, B., et al. (2020). Chemogenetic Control of Nanobodies. *Nat. Methods*. doi:10.1038/s41592-020-0746-7.

Früholz, S., Fäßler, F., Kolukisaoglu, Ü., and Pimpl, P. (2018). Nanobody-triggered lockdown of VSRs reveals ligand reloading in the Golgi. *Nat. Commun.* doi:10.1038/s41467-018-02909-6.

Gadeyne, A., Sánchez-Rodríguez, C., Vanneste, S., Di Rubbo, S., Zauber, H., Vanneste, K., et al.

(2014). The TPLATE adaptor complex drives clathrin-mediated endocytosis in plants. *Cell* 156, 691–704. doi:10.1016/j.cell.2014.01.039.

Gómez, B. G., Lozano-Durán, R., and Wolf, S. (2019). Phosphorylation-dependent routing of RLP44 towards brassinosteroid or phytosulfokine signalling. *bioRxiv*. doi:10.1101/527754.

Gu, M., Liu, Q., Watanabe, S., Sun, L., Hollopeter, G., Grant, B. D., et al. (2013). AP2 hemicomplexes contribute independently to synaptic vesicle endocytosis. *Elife* 2013, 1–21. doi:10.7554/eLife.00190.

Herberich, E., Sikorski, J., and Hothorn, T. (2010). A robust procedure for comparing multiple means under heteroscedasticity in unbalanced designs. *PLoS One*. doi:10.1371/journal.pone.0009788.

Hirst, J., Schlacht, A., Norcott, J. P., Traynor, D., Bloomfield, G., Antrobus, R., et al. (2014). Characterization of TSET, an ancient and widespread membrane trafficking complex. *Elife* 2014, 1–18. doi:10.7554/eLife.02866.001.

Ingram, J. R., Schmidt, F. I., and Ploegh, H. L. (2018). Exploiting Nanobodies' Singular Traits. *Annu. Rev. Immunol.* doi:10.1146/annurev-immunol-042617-053327.

Irani, N. G., Di Rubbo, S., Mylle, E., Van Den Begin, J., Schneider-Pizoń, J., Hniliková, J., et al. (2012). Fluorescent castasterone reveals BRI1 signaling from the plasma membrane. *Nat. Chem. Biol.* 8, 583–589. doi:10.1038/nchembio.958.

Jelínková, A., Malínská, K., and Petrášek, J. (2019). "Using FM dyes to study endomembranes and their dynamics in plants and cell suspensions," in *Methods in Molecular Biology* doi:10.1007/978-1-4939-9469-4_11.

Jelínková, A., Malínská, K., Simon, S., Kleine-Vehn, J., Pařezová, M., Pejchar, P., et al. (2010). Probing plant membranes with FM dyes: Tracking, dragging or blocking? *Plant J.* 61, 883–892. doi:10.1111/j.1365-313X.2009.04102.x.

Karimi, M., De Meyer, B., and Hilson, P. (2005). Modular cloning in plant cells. *Trends Plant Sci.* 10, 103–105. doi:10.1016/j.tplants.2005.01.008.

Kim, S. Y., Xu, Z.-Y., Song, K., Kim, D. H., Kang, H., Reichardt, I., et al. (2013). Adaptor Protein Complex 2-Mediated Endocytosis Is Crucial for Male Reproductive Organ Development in Arabidopsis. *Plant Cell*. doi:10.1105/tpc.113.114264.

Kitakura, S., Vanneste, S., Robert, S., Löfke, C., Teichmann, T., Tanaka, H., et al. (2011). Clathrin mediates endocytosis and polar distribution of PIN auxin transporters in Arabidopsis. *Plant Cell*. doi:10.1105/tpc.111.083030.

Künzl, F., Früholz, S., Fäßler, F., Li, B., and Pimpl, P. (2016). Receptor-mediated sorting of soluble vacuolar proteins ends at the trans-Golgi network/early endosome. *Nat. Plants*. doi:10.1038/NPLANTS.2016.17.

Li, X., and Pan, S. Q. (2017). Agrobacterium delivers VirE2 protein into host cells via clathrin-mediated endocytosis. *Sci. Adv.* doi:10.1126/sciadv.1601528.

Li, X., Wang, X., Yang, Y., Li, R., He, Q., Fang, X., et al. (2011). Single-Molecule Analysis of PIP2;1 Dynamics and Partitioning Reveals Multiple Modes of Arabidopsis Plasma Membrane Aquaporin Regulation. *Plant Cell* 23, 3780–3797. doi:10.1105/tpc.111.091454.

Ma, Y., Miotk, A., Šutiković, Z., Ermakova, O., Wenzl, C., Medzihradszky, A., et al. (2019). WUSCHEL acts as an auxin response rheostat to maintain apical stem cells in Arabidopsis. *Nat. Commun.* doi:10.1038/s41467-019-13074-9.

Marquès-Bueno, M. M., Morao, A. K., Cayrel, A., Platre, M. P., Barberon, M., Caillieux, E., et al. (2016). A versatile Multisite Gateway-compatible promoter and transgenic line collection for cell type-specific functional genomics in Arabidopsis. *Plant J.* doi:10.1111/tpj.13099.

Martins, S., Dohmann, E. M. N., Cayrel, A., Johnson, A., Fischer, W., Pojer, F., et al. (2015). Internalization and vacuolar targeting of the brassinosteroid hormone receptor BRI1 are regulated by ubiquitination. *Nat. Commun.* doi:10.1038/ncomms7151.

Mbengue, M., Bourdais, G., Gervasi, F., Beck, M., Zhou, J., Spallek, T., et al. (2016). Clathrin-dependent endocytosis is required for immunity mediated by pattern recognition receptor kinases. *Proc. Natl. Acad. Sci.* doi:10.1073/pnas.1606004113.

Mitsunari, T., Nakatsu, F., Shioda, N., Love, P. E., Grinberg, A., Bonifacino, J. S., et al. (2005). Clathrin adaptor AP-2 is essential for early embryonal development. *Mol. Cell. Biol.* 25, 9318–23. doi:10.1128/MCB.25.21.9318-9323.2005.

Muyldermans, S. (2013). Nanobodies: Natural Single-Domain Antibodies. *Annu. Rev. Biochem.* 82, 775–797. doi:10.1146/annurev-biochem-063011-092449.

Pasin, F., Kulasekaran, S., Natale, P., Simón-Mateo, C., and García, J. A. (2014). Rapid fluorescent reporter quantification by leaf disc analysis and its application in plant-virus studies. *Plant Methods*. doi:10.1186/1746-4811-10-22.

Rigal, A., Doyle, S. M., and Robert, S. (2015). Live cell imaging of FM4-64, a tool for tracing the endocytic pathways in Arabidopsis root cells. *Methods Mol. Biol.* doi:10.1007/978-1-4939-1902-4_9.

Robinson, M. S. (2015). Forty Years of Clathrin-coated Vesicles. *Traffic* 16, 1210–1238. doi:10.1111/tra.12335.

Robinson, M. S., Sahlender, D. A., and Foster, S. D. (2010). Rapid Inactivation of Proteins by Rapamycin-Induced Rerouting to Mitochondria. *Dev. Cell* 18, 324–331. doi:10.1016/j.devcel.2009.12.015.

Rstudio Team (2019). RStudio: Integrated development for R. RStudio, Inc., Boston MA. *RStudio*. doi:10.1007/978-3-642-20966-6.

Sánchez-Rodríguez, C., Shi, Y., Kesten, C., Zhang, D., Sancho-Andrés, G., Ivakov, A., et al. (2018). The Cellulose Synthases Are Cargo of the TPLATE Adaptor Complex. *Mol. Plant* 11, 346–349. doi:10.1016/j.molp.2017.11.012.

Schindelin, J., Arganda-Carreras, I., Frise, E., Kaynig, V., Longair, M., Pietzsch, T., et al. (2012).

Fiji: an open-source platform for biological-image analysis. *Nat. Methods*. doi:10.1038/nmeth.2019.

Schneider, C. A., Rasband, W. S., and Eliceiri, K. W. (2012). NIH Image to ImageJ: 25 years of image analysis. *Nat. Methods*.

Traub, L. M. (2019). A nanobody-based molecular toolkit provides new mechanistic insight into clathrin-coat initiation. *Elife*. doi:10.7554/elife.41768.

Van Damme, D., Coutuer, S., De Rycke, R., Bouget, F.-Y., Inze, D., and Geelen, D. (2006). Somatic Cytokinesis and Pollen Maturation in Arabidopsis Depend on TPLATE, Which Has Domains Similar to Coat Proteins. *Plant Cell Online* 18, 3502–3518. doi:10.1105/tpc.106.040923.

Wang, C., Hu, T., Yan, X., Meng, T., Wang, Y., Wang, Q., et al. (2016). Differential Regulation of Clathrin and Its Adaptor Proteins during Membrane Recruitment for Endocytosis. *Plant Physiol.* 171, 215–229. doi:10.1104/pp.15.01716.

Wang, C., Yan, X., Chen, Q., Jiang, N., Fu, W., Ma, B., et al. (2013). Clathrin Light Chains Regulate Clathrin-Mediated Trafficking, Auxin Signaling, and Development in Arabidopsis. *Plant Cell* 25, 499–516. doi:10.1105/tpc.112.108373.

Wang, P., Pleskot, R., Zang, J., Winkler, J., Wang, J., Yperman, K., et al. (2019). Plant AtEH/Pan1 proteins drive autophagosome formation at ER-PM contact sites with actin and endocytic machinery. *Nat. Commun.* doi:10.1038/s41467-019-12782-6.

Wang, S., Yoshinari, A., Shimada, T., Hara-Nishimura, I., Mitani-Ueno, N., Feng Ma, J., et al. (2017). Polar Localization of the NIP5;1 Boric Acid Channel Is Maintained by Endocytosis and Facilitates Boron Transport in Arabidopsis Roots. *Plant Cell* 29, 824–842. doi:10.1105/tpc.16.00825.

Yamaoka, S., Shimono, Y., Shirakawa, M., Fukao, Y., Kawase, T., Hatsugai, N., et al. (2013). Identification and Dynamics of Arabidopsis Adaptor Protein-2 Complex and Its Involvement in Floral Organ Development. *Plant Cell* 25, 2958–2969. doi:10.1105/tpc.113.114082.

Yeung, B. G., Phan, H. L., and Payne, G. S. (2013). Adaptor Complex-independent Clathrin Function in Yeast. *Mol. Biol. Cell* 10, 3643–3659. doi:10.1091/mbc.10.11.3643.

Yoshinari, A., Fujimoto, M., Ueda, T., Inada, N., Naito, S., and Takano, J. (2016). DRP1-dependent endocytosis is essential for polar localization and boron-induced degradation of the borate transporter BOR1 in arabidopsis thaliana. *Plant Cell Physiol.* 57, 1985–2000. doi:10.1093/pcp/pcw121.

Yoshinari, A., Hosokawa, T., Amano, T., Beier, M. P., Kunieda, T., Shimada, T., et al. (2019). Polar Localization of the Borate Exporter BOR1 Requires AP2-Dependent Endocytosis. *Plant Physiol.*, pp.01017.2018. doi:10.1104/pp.18.01017.

Zhang, Y., Yu, Q., Jiang, N., Yan, X., Wang, C., Wang, Q., et al. (2017). Clathrin regulates blue light-triggered lateral auxin distribution and hypocotyl phototropism in Arabidopsis. *Plant Cell Environ.* doi:10.1111/pce.12854.

519

520 **10 Figures**

Figure1

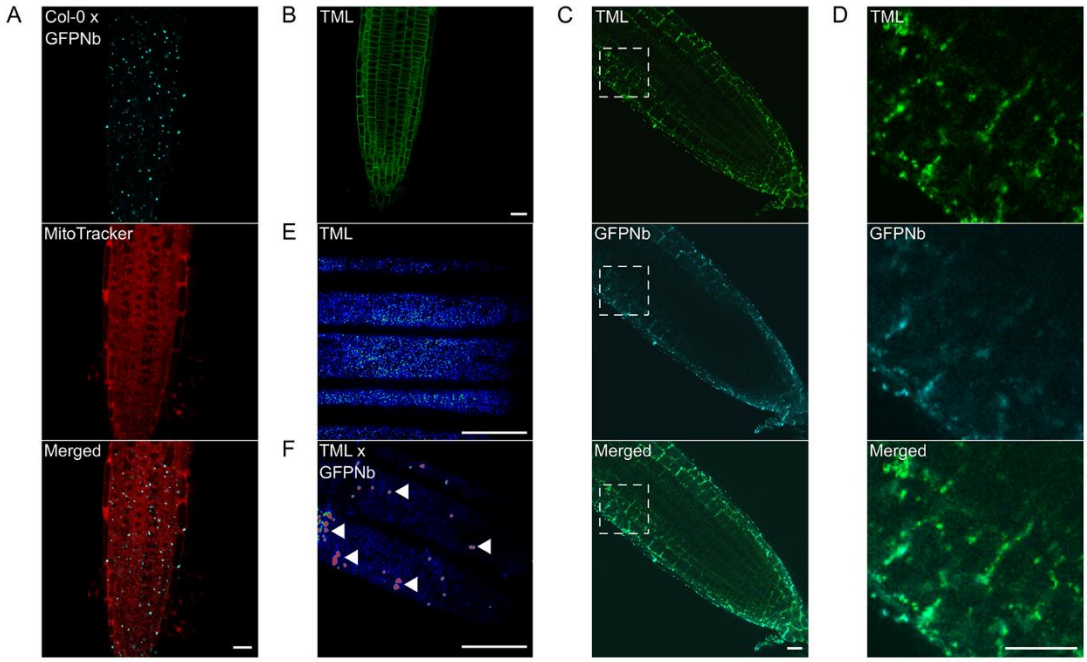

521

522 **Figure 1. Expression of a mitochondrial-targeted nanobody against GFP allows delocalization**
523 **of TML-GFP.**

524 (A) Representative image of a wild type root expressing MITOTagBFP2-GFPNb counterstained with
525 MitoTracker Red showing targeting of the construct to cytosolic punctae of various sizes, likely
526 representing dysfunctional clustered mitochondria. (B) Representative Arabidopsis root image of *tml-*
527 *1(-/-)* complemented with TML-GFP showing that the functional TML fusion is predominantly
528 targeted to the PM. (C and D) Representative overview images and respective blow-ups of the outlined
529 region of Arabidopsis roots where TML-GFP in *tml-1(-/-)* was combined with MITOTagBFP2-GFPNb
530 expression, leading to its delocalization from the PM. (E and F) Representative, rainbow intensity
531 colored, grazing sections through the PM, showing the recruitment of TML to endocytic foci without
532 (E) and with partial delocalization of TML-GFP (F, arrowheads). Scalebars equal 20 µm.

533

534

Figure 2

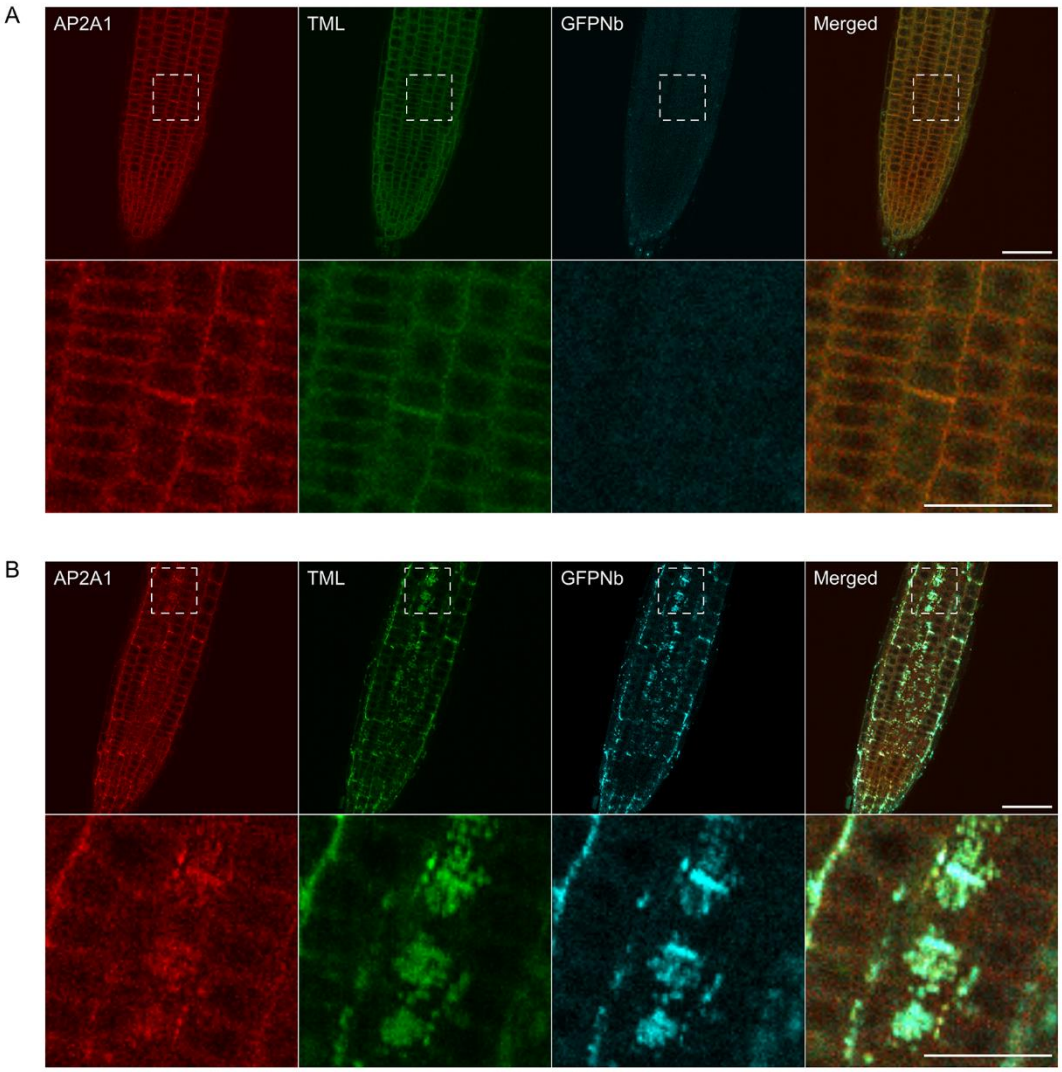

535

536 **Figure 2. Delocalization of TML also affects the targeting of other endocytic players**

537 (A and B) Representative images and blow-ups of the outlined regions of Arabidopsis roots
538 expressing TML-GFP and AP2A1-TagRFP without (A) and with (B) MITOTagBFP2-GFPNb
539 expression. GFPNb expression causes delocalization of both TML and AP2A1. Scale bars equal 20
540 µm (overview pictures) or 10 µm (blow up pictures).

541

542

543

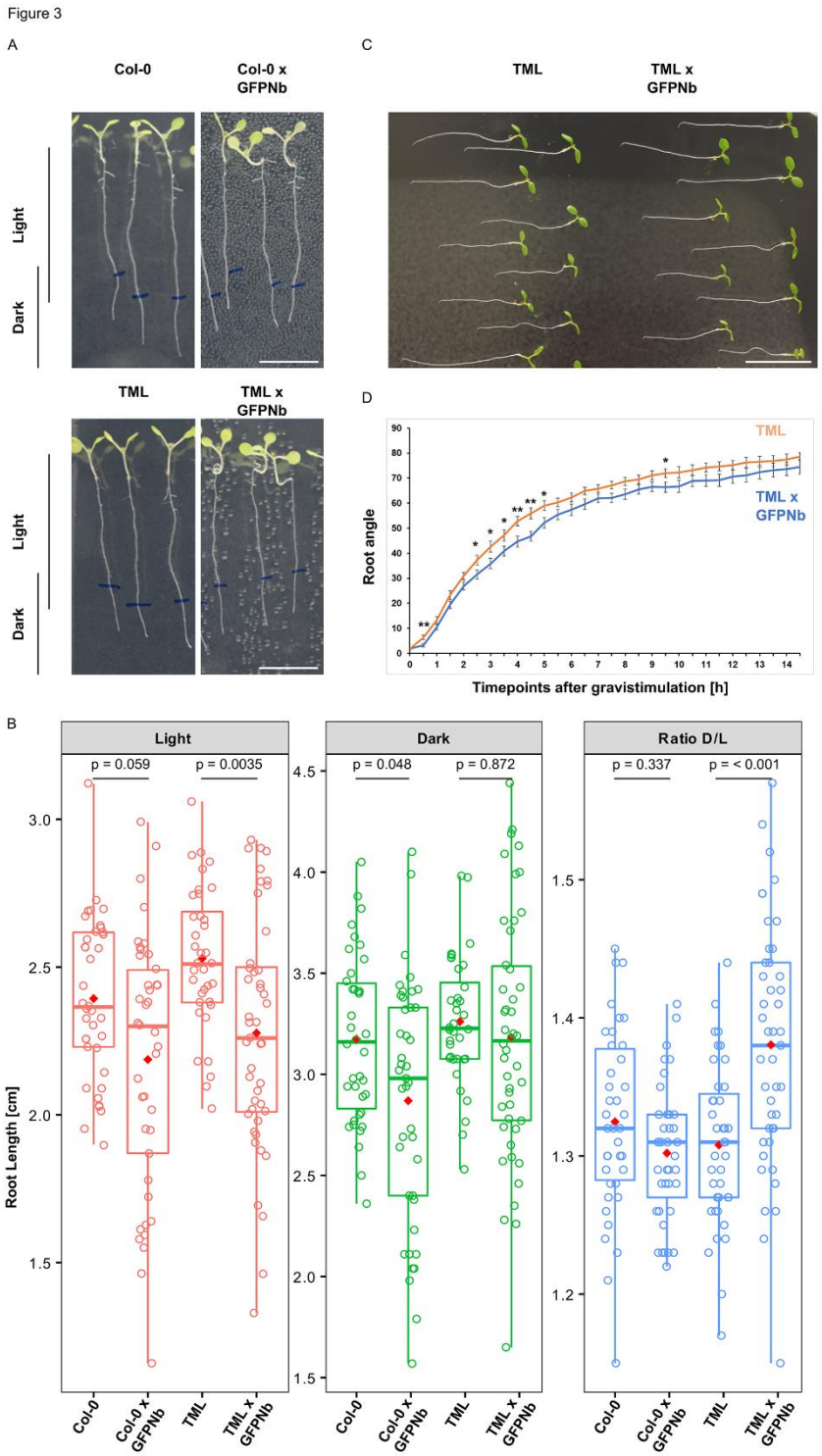

544

545 **Figure 3. Delocalizing TML-GFP in root epidermal and cortical cells has only minor effects on**
546 **root growth.**

547 (A and B) Representative seedling examples and quantification of root growth in light and continuous
548 dark comparing wild type seedlings (Col-0), wild type seedlings expressing MITOTagBFP2-GFPNb

549 (Col-0 x GFPNb), complemented *tml-1(-/-)* mutants expressing TML-GFP (TML) and complemented
550 *tml-1(-/-)* mutants expressing TML-GFP (TML) and MITOTagBFP2-GFPNb (Col-0 x GFPNb) (TML
551 x GFPNb). The quantification shows a box plot and jitter box representation (the lines represent the
552 median and the diamonds represent the mean) of individual roots (Col-0, n = 38; Col-0 x GFPNb, n =
553 39; TML, n = 39 and TML x GFPNb, n= 45) grown in continuous light and subsequently in continuous
554 dark as well as the respective dark/light ratio. The statistical significance was determined using the
555 Tukey contrasts procedure for Comparing Multiple Means under Heteroscedasticity. (C and D)
556 Representative seedling examples and quantification comparing root bending of the complemented
557 *tml-1(-/-)* line without (TML) or with GFPNb expression (TML x GFPNb; n = 20 for each genotype)
558 up to 14 hours after gravistimulation. Error bars represent standard error. Asterisks indicate statistically
559 significant differences, determined using the Wilcoxon-signed rank test (*: p<0.05; **: p<0.01). Scale
560 bars equal 1 cm.

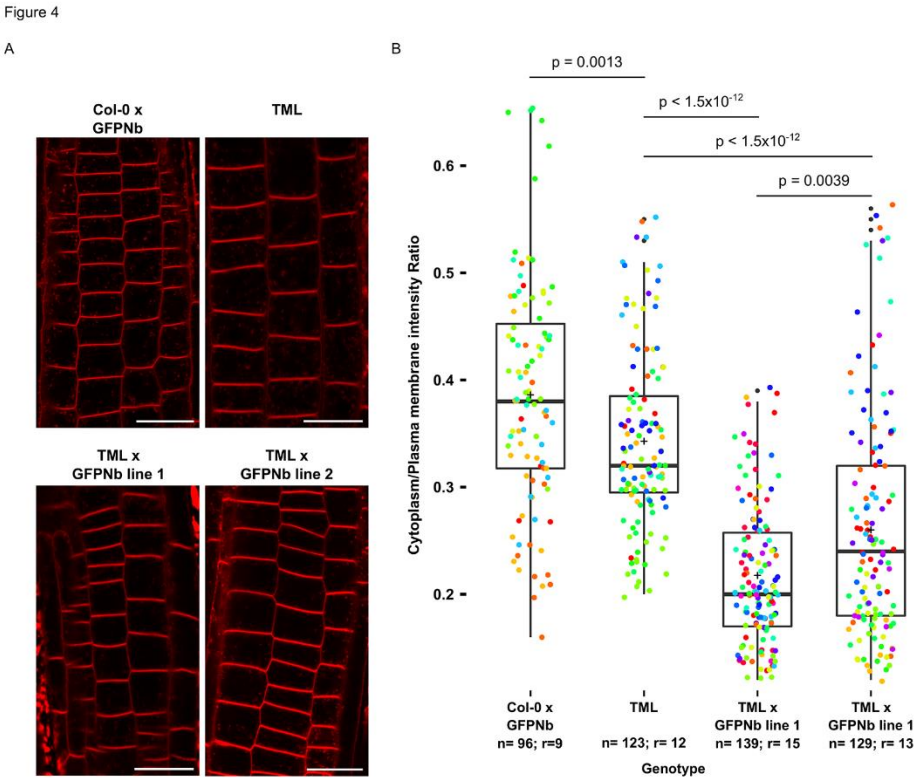

561

562 **Figure 4. Nanobody-dependent delocalization reduces endocytic flux.**

563 (A) Representative single confocal slices of FM4-64 stained root cells of the different lines for which
564 endocytic flux was quantified. FM4-64 uptake was compared between wild type Arabidopsis
565 expressing MITOTagBFP2-GFPNb (Col-0 x GFPNb), the TML-GFP expressing complemented *tml-*

1(-/-) mutant (TML), and two independent lines of the TML-GFP expressing complemented *tml-1(-/-)* mutant expressing MITOTagBFP2-GFPNb (TML x GFPNb). Scale bars equal 20 µm. (B) Box plot and Jitter box representation of the quantification of the cytoplasm/plasma membrane intensity of FM4-64 as proxy for endocytic flux. The black lines represent the median and the crosses represent the mean values. The dots represent individual measurements of cells. The rainbow-colored indication of the dots groups the cells from the different roots that were analyzed. The number of cells (n) and the number of individual roots (r) are indicated on the graph. The indicated p values were calculated using the Wilcoxon-signed rank test.